High multiplicity processes at NLO with BlackHat and Sherpa

Zvi Bern, Kemal Ozeren

Department of Physics and Astronomy, UCLA, Los Angeles, CA 90095-1547, USA
E-mail: bern@physics.ucla.edu, ozeren@physics.ucla.edu

Lance J. Dixon, Stefan Höche

SLAC National Accelerator Laboratory, Stanford University, Stanford, CA 94309, USA
E-mail: lance@slac.stanford.edu, shoeche@slac.stanford.edu

Fernando Febres Cordero

Departamento de Física, Universidad Simón Bolívar, Caracas 1080A, Venezuela
E-mail: ffebres@usb.ve

Harald Ita∗

Albert-Ludwigs-Universität Freiburg, Physikalisches Institut, D-79104 Freiburg, Germany
E-mail: harald.ita@physik.uni-freiburg.de

David Kosower

Institut de Physique Théorique, CEA–Saclay, F–91191 Gif-sur-Yvette cedex, France
E-mail: david.kosower@cea.fr

Daniel Maître∗

Theory Division, Physics Department, CERN, CH–1211 Geneva 23, Switzerland
Department of Physics, University of Durham, DH1 3LE, UK
E-mail: daniel.maitre@durham.ac.uk

In this contribution we review recent progress with fixed-order QCD predictions for the production of a vector boson in association with jets at hadron colliders, using the programs BLACKHAT and SHERPA. We review general features of next-to-leading-order (NLO) predictions for the production of a massive vector boson in association with four jets. We also discuss how precise descriptions of vector-boson production can be applied to the determination of backgrounds to new physics signals. Here we focus on data-driven backgrounds to a missing-energy-plus-jets search performed by CMS. Finally, we review recent progress in developing theoretical tools for high-multiplicity loop-computation within the BLACKHAT-library. In particular, we discuss methods for handling the color degrees of freedom in multi-jet predictions at NLO.

∗Speaker.

1. Introduction

The production of a massive vector boson in association with jets is an important process at hadron colliders. The cross sections are large, the events are relatively clean, and they form significant backgrounds to many interesting physics signals. Because these processes are so well understood, both experimentally and theoretically, they are widely used to validate or test new tools and methods.

The last few years have seen continued progress in the perturbative description of high-multiplicity processes. The next-to-leading order (NLO) QCD corrections for $W + 4$-jet production at hadron colliders were completed in 2011 [1, 2], followed by the calculation of the same process with a W boson replaced by a Z boson [3]. At this conference we have shown preliminary results for the $W + 5$-jet process. All these fixed-order QCD predictions have been obtained using of BLACKHAT [4] and SHERPA [5, 6, 7, 8]. There has also been a lot of progress in the computation of processes with a W and Z boson accompanied by jets at NLO accuracy, matched to a parton shower (see e.g. references in ref. [9]). For such computations the high-multiplicity virtual matrix elements in QCD are a key ingredient, some of which have become available only recently. The production of $W + 2$ jets has been computed using aMC@NLO [9]. Virtual matrix elements provided by BLACKHAT have been used by different groups for such computations. The Sherpa implementation of the MC@NLO [10] approach computes W boson production in association to up to three jets [11] using virtual matrix elements from refs. [12, 13]. The POWHEG BOX [14, 15] has been used recently to compute the $Z + 2$-jet process at NLO, matched with a parton shower [16], with the virtual matrix elements [17, 18] also employed in ref. [19].

NLO predictions improve the leading order (LO) results in various ways. NLO results show a reduced dependence on the unphysical renormalization and factorization scales, as compared to LO results. This improvement becomes more significant as the number of jets and, thus, the order in the strong coupling α_s, increases. Further benefits include a better description of initial and final state radiation. The shapes of many kinematical distributions are better described at NLO. The precision offered by NLO calculations is needed for both the signal and background processes. 'Data-driven' methods very often rely on theory input for cross section ratios, in order to extrapolate backgrounds from a control region into a signal region for the same process, or to extrapolate from one process to a related process. NLO computations can also improve the theoretical precision for such ratios.

We address here several new developments in fixed-order NLO computations of vector-boson production. First, we discuss the production of a massive vector boson in association with four jets at NLO as a signal at the LHC. Next, we discuss an application of NLO computations of vector-boson production to background estimation in searches for supersymmetry. Finally, we report on some technical developments that have been important ingredients in our latest multi-jet computations.

2. $W + 4$-jet and $Z + 4$-jet predictions

We present results here for $W + 4$-jet and $Z + 4$-jet production, for which we have used

BLACKHAT [4] for both the virtual matrix elements and real-emission matrix elements. SHERPA [5, 6, 7, 8] was used for the remaining pieces (Born and subtraction), as well as for the integration over the phase space. For both processes, the calculation of the real-emission tree amplitudes is extremely challenging. In BLACKHAT, they are computed using on-shell recursion relations [20] as well as compact analytic formulae given in refs. [21, 22].

In figure 1 we display the transverse-momentum (p_T) distribution of the first, second, third and fourth jets in $Z + 4$-jet events, with the decay to a lepton pair included. We have used $\hat{H}'_T/2$ as a central choice for both the factorization scale μ_F and renormalization scale μ_R, where $\hat{H}'_T = E_T^Z + \sum_i p_T^i$ and $E_T^Z = \sqrt{M_Z^2 + \left(p_T^{e^+e^-}\right)^2}$. The sum runs over all partons. A detailed list of the cuts, jet algorithm and parameters can be found in ref. [3]. To suppress the virtual-photon component, we apply a cut on the lepton invariant mass, requiring $66\,\text{GeV} < M_{e^+e^-} < 116\,\text{GeV}$. Although the interference between Z boson and photon exchange is very small with this cut, we include it for completeness. For the virtual part we use a leading-color approximation, which has been demonstrated in refs. [13, 19, 2] to be good to about three percent, as discussed further in section 4.2.

In the top pane of figure 1, the blue and black curves are the central LO and NLO predictions, respectively. In the middle pane the ratio is taken with respect to the central NLO result. Scale variation bands are displayed in orange for the LO and in gray for the NLO result. They are obtained as the envelope from varying $\mu = \mu_R = \mu_F$ by factors of $1/2$, $1/\sqrt{2}$, 1, $\sqrt{2}$ and 2 around the central scale value. The bottom pane displays the ratio of the $Z + 4$-jet distributions with respect to the $W^\pm + 4$-jet ones, both at leading order and next-to-leading order. In contrast to the individual distributions, the ratios do not suffer from large NLO corrections. The shape of the Z/W^- ratio is explained by the dominance of the valence distributions, particularly $u(x)$, at large x. The Z has a significant coupling to the u quark, while the W^- couples only to the d quark, among the valence quarks. As the jet p_T increases, parton-distribution functions (PDF's) of higher x are probed, where $u(x)/d(x)$ rises. The Z/W^+ ratio is flat because both the W and Z couplings are dominated by the coupling to the same $u(x)$ PDF. These sorts of ratios are very useful in data-driven methods.

The shape differs significantly between the central LO and NLO predictions for the p_T distributions of the first, second and third jets. The scale variation is, as expected, much smaller at NLO than it is at LO.

3. Z/γ ratios

The production of jets in association with a Z boson that decays into a neutrino pair is an irreducible background for missing energy plus jets (METJ) searches. Missing energy signals arise from the production of new particles that escape the detector unobserved. A typical example is the lightest supersymmetric particle (LSP) in R-parity conserving models of supersymmetry. As it is an irreducible background, the impact of the $Z(\to \nu\nu) + $jets processes (METZJ) must be estimated carefully. Typically data-driven methods are used with only ratios provided by theory. There are several strategies to estimate this background (see e.g. refs. [23, 24, 25, 26]), using related processes in which the production of the Z boson and its subsequent decay into neutrinos is replaced by a more accessible signature:
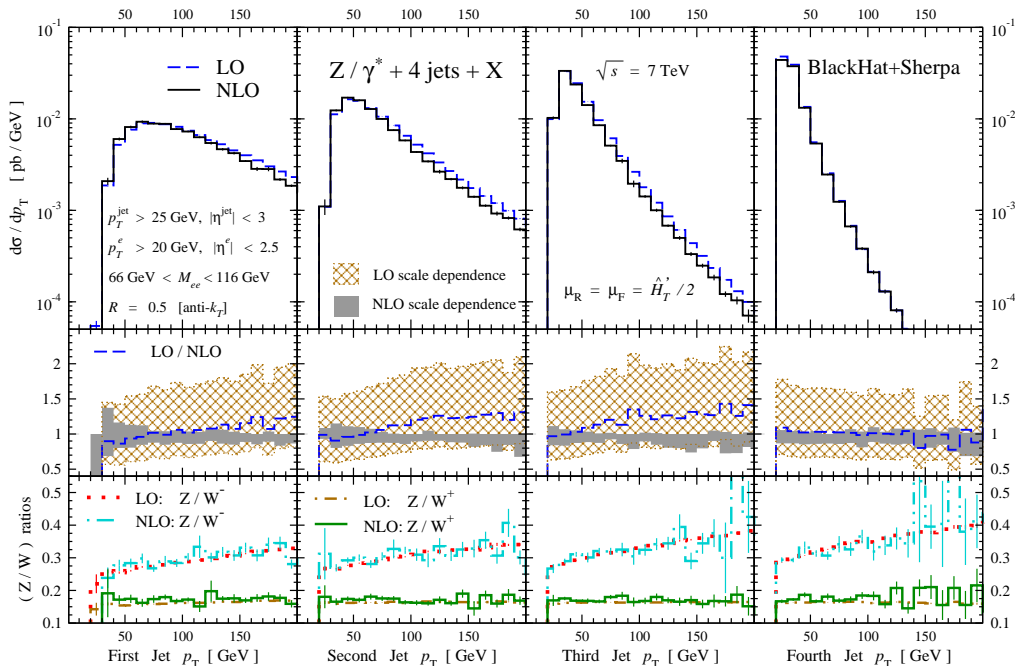
Figure 1: Distribution in p_T for the first, second, third and fourth jets in $Z + 4$-jet events.

- $Z\,(\to ll)$+jets. The advantage of this process is that the production dynamics are very similar to the one in the neutrino process. However, the statistics is smaller than $Z \to \nu\nu$ by a factor of six for each lepton flavor, and is further reduced by the experimental acceptance and identification efficiency for each charged lepton.

- $W\,(\to l\nu)$+jets. This process has a cross section higher by a factor of six, but suffers from contamination from $t\bar{t}$, and potentially, from the new physics one aims to measure.

- γ+jets. Replacing the Z decay to neutrinos by a photon yields a cross section higher by a factor of four to five, but the production dynamics are different and a reliable theory prediction is needed to obtain a solid conversion factor.

Here we present NLO calculations of the ratios needed for the photon-based estimation strategy. The CMS collaboration has studied and used [23, 24] W-boson and photon production in association with jets to estimate METZJ backgrounds [24, 26]. Photon production in association with jets has also been studied in ref. [25] and used by the ATLAS collaboration [27] in their data-driven estimates of the METZJ background.

Partonic calculations involving photons develop infrared singularities when the photon is emitted collinear to a quark. These divergences can be avoided by imposing a standard cone isolation for the photon. However, this strategy requires the use of photon fragmentation functions which are extracted from data and are not known very precisely. Another approach, proposed by Frixione [28], removes the need for the fragmentation functions but is difficult to implement in an experimental measurement. For the estimation of the ratio of $\gamma + 2$ jets to $Z + 2$ jets we use the Frixione isolation. We estimate the difference between this isolation and the CMS cone isolation using a
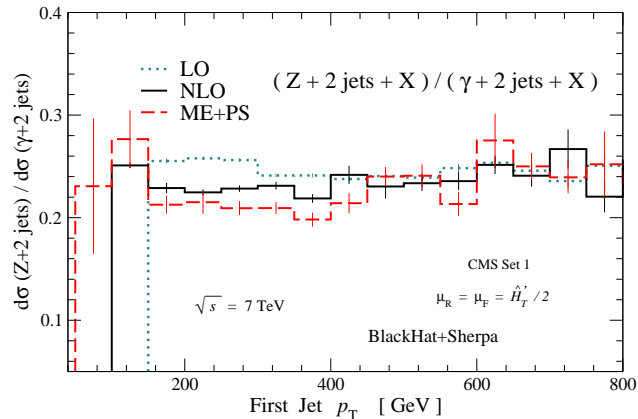
Figure 2: Ratio of the p_T distribution of the first jet in $Z + 2$-jet and $\gamma + 2$-jet production. The dotted blue line represents the LO ratio, the solid black line the NLO result, while the ME+PS result is represented by the dashed red line.

code by Gordon and Vogelsang [29] and JetPhox [30, 31]. We find that the difference between the standard cone isolation and Frixione's isolation is small, and decreases as the transverse energy of the photon increases, which is the case of interest for this study. For more details we refer to ref. [32].

The estimation of uncertainties on our result for the ratios (as for most NLO predictions for ratios) is difficult. The commonly used method of varying the renormalization and factorization scales yields a very small estimate, because most of the scale-dependence is correlated between the numerator and denominator. A similar effect occurs for the PDF-error propagation. To estimate the error, we computed the ratio using the matrix-element-matched-to-parton-shower (ME+PS) method of SHERPA. We took the difference between the NLO and ME+PS ratios as an estimate of the uncertainty of our result. An example of such a ratio, for cuts relevant to a CMS search using the 2010 LHC data [24], is shown in Figure 2 as a function of the p_T of the first jet. The NLO and ME+PS predictions for the Z to γ ratio track each other well across the whole range of jet p_T. Other observables exhibit similar behavior [32], leading to the conclusion that the photon-plus-jets process gives a good handle on the $Z \to \nu\nu$ background.

We have recently extended this computation [33] to the ratio of $Z + 3$-jet to $\gamma + 3$-jet production. This work was also instigated by the CMS collaboration [23] to help them estimate the uncertainty in the $Z \to \nu\nu$ background to new physics searches, in particular for the more stringent cuts used in analyzing the 2011 LHC data [26]. We have computed the ratio of the two processes for different sets of cuts on two kinematic variables H_T^{jets} and MET^{jets}. H_T^{jets} is defined as the sum of the transverse energy of jets with $p_T > 50$ GeV and $|\eta| < 2.5$, while MET^{jets} is defined as the modulus of the vectorial sum of the transverse momenta of the jets with $p_T > 30$ GeV and $|\eta| < 5$.

The scale Q of the cuts on H_T^{jets} and MET^{jets} in the analysis is large enough that one may worry about large logarithms of the form $\log(Q/p_T^{\min})$. One way of assessing whether these logarithms are large is to look at the ratio of $Z + 3$ jets over $Z + 2$ jets. A value too close to one could result from large logarithms spoiling the perturbative expansion. Figure 3 shows this ratio as a function of H_T^{jets} and $H_T^{\text{jets}} - MET^{\text{jets}}$. In regions where this ratio is close to one, we cannot be sure about
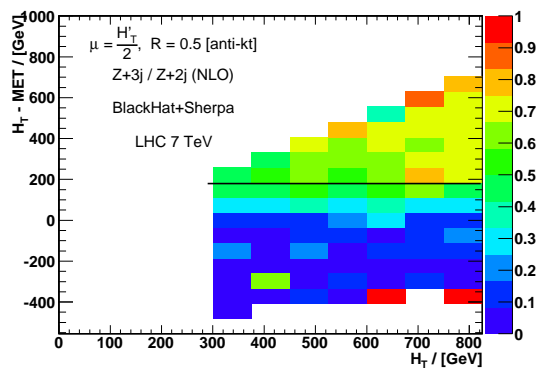
Figure 3: Ratio of the $Z + 3$ to $Z + 2$ jets ratio as a function of H_T^{jets} and $H_T^{\text{jets}} - MET^{\text{jets}}$.

the validity of the perturbative expansion. Such large effects may nonetheless largely cancel out in Z+jets/γ+jets ratios, leaving those predictions reliable in spite of them. It is worth noting that the validity of the NLO prediction in these regions, where the perturbative expansion might be unreliable, can be tested experimentally by measuring such ratios in the γ+jets samples.

We find that the theoretical uncertainty on the conversion between photons and Z bosons is less than 10% for events with either two or three associated jets, allowing the photon channel to provide an excellent determination of the Standard Model missing-E_T +jets background.

4. Color Automation

Scattering processes at hadron colliders are dominated by the strong interactions. The previously-discussed processes of vector-boson production in association with jets are typical examples. For events with kinematics in the perturbative regime, cross sections and distributions can be predicted from first principles, allowing detailed comparisons between theory and experiment. To this end we focus on the precise perturbative description of the interactions of colored partons within quantum-field theory.

The Lagrangian interaction terms of colored fields make perturbative computations very chal-lenging. A successful computational strategy disentangles the various dynamical degrees of free-dom, such as kinematics, spin and color quantum numbers. Targeted algorithms can then be de-vised to deal efficiently with the components of the computation. This approach is realized in many matrix-element generators and has been particularly useful for recent multi-jet computations at NLO. Alternatively, one can treat color simultaneously with the kinematic variables [34]. This method, implemented as a Berends-Giele recursion [35], is similar to methods used in other auto-mated LO computations [36, 37, 38, 39].

In BLACKHAT we separate color and kinematic degrees of freedom early on. We then compute color-ordered tree- and loop-level objects, so-called primitive amplitudes. These amplitudes are assembled into the full matrix elements only at the end of the computation. The required color weights and interference matrix are precomputed. We use modern on-shell and unitarity techniques in order to compute the color-ordered building blocks: tree amplitudes and, subsequently, loop amplitudes.

Focusing on these particular color-ordered objects has several benefits. First of all, these components have a simpler analytic structure than the full amplitude; for example, they depend on a reduced set of kinematic invariants. This property implies that a smaller number of unitarity cuts needs to be computed in an on-shell approach. The simpler analytic structure also leads to improved numerical stability of the amplitudes.

The second main benefit of the color-ordered approach is that it can be exploited to yield significant efficiency gains in the numerical phase-space integration [13]. If we consider the number of quark flavors n_f to be of the same order as the number of colors N_c, and take the limit as both become large, then the color-summed (virtual) cross section can be expanded in powers of $1/N_c^2$. The $1/N_c^2$-suppressed terms are numerically quite small. Thus, for a fixed integration error, fewer evaluations are needed for these parts of the cross section. That is, for most phase-space points only a small subset of all color-ordered amplitudes must be computed, namely those that contribute to the leading-color term in the cross section.

In this talk we discuss a method to automate the color-ordered approach in loop computations. The key question is: how we can express generic matrix elements as linear combinations of color-ordered objects. We also discuss the quantitative impact of subleading-color terms on differential cross sections. In particular, we consider the distribution of the fourth jet p_T in the state-of-the-art NLO results for $W + 4$-jet production [13, 1, 2].

4.1 Partial amplitudes from primitive amplitudes.

The standard "trace-based" color decomposition of a one-loop QCD amplitude is into a set of color structures involving traces or open strings of $N_c \times N_c$ $SU(N_c)$ generator matrices T^{a_k}, one for each external gluon. The open strings terminate on fundamental indices corresponding to the external quarks and antiquarks in the process. The coefficients of these color structures are called partial amplitudes. The partial amplitudes are in turn built from color-ordered primitive amplitudes, but the precise relations can be laborious to determine in the general case. The aim of this section is to describe an algorithm [2] for determining these relations.

For many specific processes, the decomposition of the one-loop matrix elements and the color-summed virtual cross sections in terms of primitive amplitudes is well known. The explicit color decompositions of all-n matrix elements of purely gluonic processes can be found in refs. [40, 41] and the ones with a single of quark line in ref. [42]. Furthermore, the decomposition of the four-quark amplitude was given in refs. [43, 17, 18] and that of the four-quark process with an additional gluon in [44, 45]. The decomposition of QCD scattering amplitudes with six and seven partons, including either four or six quarks, have been given only recently, using the algorithm reviewed here [2].

The algorithm is based on analyzing Feynman diagrams and their inherent color information. We consider a specific subprocess in QCD. We generate the full set of Feynman diagrams of the colored loop amplitude. Next, we associate a linear combination of Feynman diagrams to partial amplitudes. To this end, we dress Feynman diagrams with color matrices and sum over repeated (internal) color indices. Partial amplitudes are defined as coefficients of particular products of color matrices. Feynman diagrams are associated with a given partial amplitude if they contribute to its defining color structure. Simple factors (powers of N_c, signs and integers) are generated by the

color-index summation, and these factors enter the relation between each Feynman diagram and each partial amplitude to which it contributes.

In a second step, we associate a linear combination of Feynman diagrams with primitive amplitudes. To do this, we again dress Feynman diagrams with color matrices; however, this time we associate adjoint representation color charges to quarks as well as gluons. Again we sum over the internal color indices. We define the primitive amplitudes as the leading-color single-trace partial amplitudes [40] for a given cyclic ordering of the external gluons and (adjoint) quarks. A primitive amplitude is thus associated with the Feynman diagrams that contribute to a particular single-trace color structure. For further details, and refinements when dealing with quark lines, we refer the reader to the original literature [40, 41, 42, 2].

Once we have the explicit expressions of both the partial amplitudes and the primitive amplitudes in terms of linear combinations of Feynman diagrams, we can manipulate these two sets of equations. We express the partial amplitudes in terms of the primitive amplitudes by solving the linear set of equations to eliminate the explicit dependence on the individual Feynman diagrams. In this step, we observe a redundancy of the linear equations we have to solve. This redundancy implies that certain linear combinations of primitive amplitudes add up to zero. That is, we find non-trivial relations between primitive amplitudes. Thus, we may find a set of equivalent color decompositions of a given partial amplitude.

We point out some key features of the implementation of the above algorithm. Because it is based on Feynman diagrams, the algorithm is limited in parton multiplicity due to the rapid growth in the number of diagrams. (However, the algorithm only has to be performed once and for all for a given process, not each time an amplitude is evaluated.) We find that there is no serious obstruction to carrying out the decomposition for processes with up to eight external partons. Processes with zero or two external quarks are computationally the most challenging; however, explicit formulas are known for these cases. In addition, it turns out that many diagrams (e.g. diagrams involving four-gluon interactions) may be dropped from the start, significantly reducing the computational load. For an efficient implementation, we find it convenient to use QGRAF [46] for diagram generation and the computer algebra package FORM [47] for summing over internal color indices.

We conclude this section with a brief discussion of the relations between primitive amplitudes, which appear as a byproduct of the above algorithm. At low multiplicity, one can identify the anti-symmetry of the color-ordered gluon-quark-quark vertex as the origin of the relations between primitive amplitudes. Explicit examples of this may be found in ref. [2]. The relations obtained between primitive amplitudes can be used to optimize caching, and thus, how long the subleading-color contributions take to evaluate numerically. Finally, it seems likely that understanding the relations between primitive amplitudes will help to establish all-n formulae for the color decompositions. We have not explored this direction further.

4.2 Quantitative impact of subleading-color terms.

We now discuss the quantitative impact of subleading-color terms on NLO predictions. We focus on the distribution in the fourth jet p_T in $W + 4$-jet production at the LHC, since it is a key observable. Predictions of jet p_T-distributions have already been given in ref. [1]. In that work a leading-color approximation was used for the virtual parts; the remaining real, Born and subtraction terms were computed to all orders in the color expansion. Here we show results including the
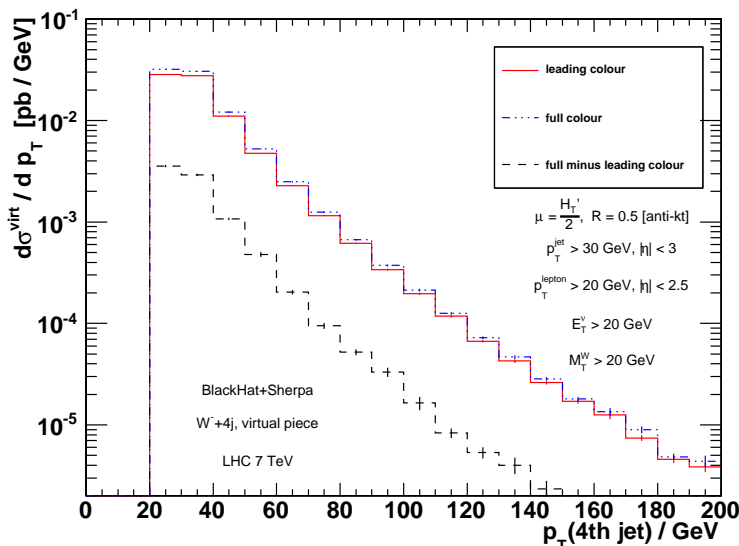
Figure 4: A comparison of the full and leading-color virtual contributions to the p_T distribution of the fourth jet in W^-+4-jet production at the 7 TeV LHC.

remaining subleading-color corrections [2]. The systematics we observe match our earlier results on subleading-color contributions to $W + 3$-jet production [13].

We use the same basic setup of matrix-element generators, Monte Carlo integration, scale choices and cuts as discussed in section 2. There is no unique definition of the leading-color terms; definitions may differ by reassigning subleading-color terms. A detailed discussion of the leading-color approximation we use here is provided in ref. [2].

In figure 4 we compare the full-color versus leading-color virtual contributions to the p_T distribution of the fourth jet in W^-+4-jet production. Also displayed are the subleading-color contributions by themselves, labeled as 'full-minus-leading-color'. In order to obtain the full parton level differential cross section one must add the real and Born contributions in the usual way. The size of these contributions have been given recently [1, 13]; the leading-color virtual part accounts for about 20% of the cross section.

Figure 4 confirms that the subleading-color contribution is suppressed uniformly by almost a factor of 10 over the displayed range of p_T. The suppression appears consistent with the expected factor of $1/N_c^2$ with $N_c = 3$. With the leading-color virtual part accounting for about 20% of the total cross section, the subleading-color virtual part amounts to less than a 3% correction to the total.

A possible exception to the uniform suppression would be near a zero of the leading-color virtual cross section. Such zeros are not excluded on general grounds, but they would have to survive the sum over a large number of different helicity configurations. A priori, there is no reason to assume that the vanishing of the leading-color contribution forces also the vanishing of the subleading-color contribution. Close to a putative zero of the leading-color contribution we would expect a relative enhancement of the subleading-color piece in the virtual matrix elements. Even if

a zero were to appear in a special kinematic configuration, the subleading-color virtual terms are expected to keep their relative size with respect to the more inclusive total cross section and typical differential cross sections. Certainly figure 4 does not show any evidence for suppression of the leading-color cross section.

Although the leading-color results could point to kinematic configurations where subleading-color contributions might dominate the virtual matrix elements, only their explicit knowledge allows to determine their impact on the full cross section. Similarly, the size and uniformity of the subleading-color terms justifies the use of leading-color approximations for many multi-jet observables. Nevertheless, explicit computations are of great importance for a definitive understanding of such multi-jet observables.

Acknowledgements

References

[1] C. Berger *et al.*, *Precise predictions for W + 4-jet production at the Large Hadron Collider*, *Phys.Rev.Lett.* **106** (2011) 092001, [1009.2338].

[2] H. Ita and K. Ozeren, *Colour decompositions of multi-quark one-loop QCD amplitudes*, *JHEP* **1202** (2012) 118, [1111.4193].

[3] H. Ita *et al.*, *Precise predictions for Z + 4 jets at hadron colliders*, *Phys.Rev.* **D85** (2012) 031501, [1108.2229].

[4] C. Berger *et al.*, *An automated implementation of on-shell methods for one-loop amplitudes*, *Phys.Rev.* **D78** (2008) 036003, [0803.4180].

[5] T. Gleisberg *et al.*, *SHERPA 1.α: A proof of concept version*, *JHEP* **0402** (2004) 056, [hep-ph/0311263].

[6] T. Gleisberg *et al.*, *Event generation with SHERPA 1.1*, *JHEP* **0902** (2009) 007, [0811.4622].

[7] F. Krauss, R. Kuhn, and G. Soff, *AMEGIC++ 1.0: A Matrix element generator in C++*, *JHEP* **0202** (2002) 044, [hep-ph/0109036].

[8] T. Gleisberg and F. Krauss, *Automating dipole subtraction for QCD NLO calculations*, *Eur.Phys.J.* **C53** (2008) 501, [0709.2881].

[9] R. Frederix *et al.*, *aMC@NLO predictions for W j j production at the Tevatron*, *JHEP* **1202** (2012) 048, [1110.5502].

[10] S. Frixione and B. R. Webber, *Matching NLO QCD computations and parton shower simulations*, *JHEP* **0206** (2002) 029, [hep-ph/0204244].

[11] S. Hoeche, F. Krauss, M. Schonherr, and F. Siegert, *W + n-jet predictions with MC@NLO in Sherpa*, 1201.5882.

[12] C. Berger *et al.*, *Precise predictions for W + 3-jet production at hadron colliders*, *Phys.Rev.Lett.* **102** (2009) 222001, [0902.2760].

[13] C. Berger *et al.*, *Next-to-leading order QCD predictions for W + 3-jet distributions at hadron colliders*, *Phys.Rev.* **D80** (2009) 074036, [0907.1984].

[14] P. Nason, *A new method for combining NLO QCD with shower Monte Carlo algorithms*, *JHEP* **0411** (2004) 040, [hep-ph/0409146].

[15] S. Frixione and B. R. Webber, *Matching NLO QCD computations and parton shower simulations*, *JHEP* **0206** (2002) 029, [hep-ph/0204244].

[16] E. Re, *NLO corrections merged with parton showers for Z + 2 jets production using the POWHEG method*, 1204.5433.

[17] Z. Bern, L. J. Dixon, D. A. Kosower, and S. Weinzierl, *One-loop amplitudes for* $e^+e^- \to \bar{q}q\bar{Q}Q$, *Nucl.Phys.* **B489** (1997) 3, [hep-ph/9610370].

[18] Z. Bern, L. J. Dixon, and D. A. Kosower, *One-loop amplitudes for* e^+e^- *to four partons*, *Nucl.Phys.* **B513** (1998) 3, [hep-ph/9708239].

[19] C. Berger *et al.*, *Next-to-leading order QCD predictions for* $Z, \gamma^* + 3$-jet distributions at the Tevatron, *Phys.Rev.* **D82** (2010) 074002, [1004.1659].

[20] R. Britto, F. Cachazo, B. Feng, and E. Witten, *Direct proof of tree-level recursion relation in Yang-Mills theory*, *Phys.Rev.Lett.* **94** (2005) 181602, [hep-th/0501052].

[21] J. Drummond, J. Henn, G. Korchemsky, and E. Sokatchev, *Dual superconformal symmetry of scattering amplitudes in* $\mathcal{N} = 4$ *super-Yang-Mills theory*, *Nucl.Phys.* **B828** (2010) 317, [0807.1095].

[22] L. J. Dixon, J. M. Henn, J. Plefka, and T. Schuster, *All tree-level amplitudes in massless QCD*, *JHEP* **1101** (2011) 035, [1010.3991].

[23] **CMS** Collaboration, *Data-driven estimation of the invisible Z background to the SUSY MET plus jets search*, *CMS-PAS-SUS-08-002* (2009).

[24] **CMS** Collaboration, S. Chatrchyan *et al.*, *Search for New Physics with Jets and Missing Transverse Momentum in pp collisions at* $\sqrt{(s)} = 7$ *TeV*, *JHEP* **1108** (2011) 155, [1106.4503].

[25] S. Ask, M. Parker, T. Sandoval, M. Shea, and W. Stirling, *Using* γ+*jets production to calibrate the Standard Model* $Z(\to \nu\nu)$+*jets background to new physics processes at the LHC*, *JHEP* **1110** (2011) 058, [1107.2803].

[26] **CMS** Collaboration, S. Chatrchyan *et al.*, *Search for new physics in the multi-jet and missing transverse momentum final state in proton-proton collisions at* $\sqrt{s} = 7$ *TeV*, 1207.1898.

[27] **ATLAS** Collaboration, G. Aad *et al.*, *Search for squarks and gluinos using final states with jets and missing transverse momentum with the ATLAS detector in* $\sqrt{s} = 7$ *TeV proton-proton collisions*, *Phys.Lett.* **B710** (2012) 67, [1109.6572].

[28] S. Frixione, *Isolated photons in perturbative QCD*, *Phys.Lett.* **B429** (1998) 369, [hep-ph/9801442].

[29] L. Gordon and W. Vogelsang, *Polarized and unpolarized isolated prompt photon production beyond the leading order*, *Phys.Rev.* **D50** (1994) 1901.

[30] S. Catani, M. Fontannaz, J. Guillet, and E. Pilon, *Cross-section of isolated prompt photons in hadron hadron collisions*, *JHEP* **0205** (2002) 028, [hep-ph/0204023].

[31] P. Aurenche, M. Fontannaz, J.-P. Guillet, E. Pilon, and M. Werlen, *A new critical study of photon production in hadronic collisions*, *Phys.Rev.* **D73** (2006) 094007, [hep-ph/0602133].

[32] Z. Bern *et al.*, *Driving missing data at next-to-leading order*, *Phys.Rev.* **D84** (2011) 114002, [1106.1423].

[33] Z. Bern *et al.*, *Missing energy and jets for supersymmetry searches*, 1206.6064.

[34] C. Duhr, S. Hoeche, and F. Maltoni, *Color-dressed recursive relations for multi-parton amplitudes*, *JHEP* **0608** (2006) 062, [hep-ph/0607057].

[35] F. A. Berends and W. Giele, *Recursive calculations for processes with n gluons*, *Nucl.Phys.* **B306** (1988) 759.

[36] F. Caravaglios and M. Moretti, *An algorithm to compute Born scattering amplitudes without Feynman graphs*, *Phys.Lett.* **B358** (1995) 332, [hep-ph/9507237].

[37] A. Kanaki and C. G. Papadopoulos, *HELAC: A package to compute electroweak helicity amplitudes*, *Comput.Phys.Commun.* **132** (2000) 306, [hep-ph/0002082].

[38] M. Moretti, T. Ohl, and J. Reuter, *O'Mega: An optimizing matrix element generator*, hep-ph/0102195.

[39] T. Gleisberg and S. Hoeche, *Comix, a new matrix element generator*, *JHEP* **0812** (2008) 039, [0808.3674].

[40] Z. Bern and D. A. Kosower, *Color decomposition of one-loop amplitudes in gauge theories*, *Nucl.Phys.* **B362** (1991) 389.

[41] Z. Bern, L. J. Dixon, D. C. Dunbar, and D. A. Kosower, *One loop n-point gauge theory amplitudes, unitarity and collinear limits*, *Nucl.Phys.* **B425** (1994) 217, [hep-ph/9403226].

[42] Z. Bern, L. J. Dixon, and D. A. Kosower, *One-loop corrections to two-quark three-gluon amplitudes*, *Nucl.Phys.* **B437** (1995) 259, [hep-ph/9409393].

[43] Kunszt, Zoltan and Signer, Adrian and Trócsányi, Zoltan, *One loop helicity amplitudes for all* $2 \to 2$ *processes in QCD and* $\mathcal{N} = 1$ *supersymmetric Yang-Mills theory*, *Nucl.Phys.* **B411** (1994) 397, [hep-ph/9305239].

[44] Kunszt, Zoltan and Signer, Adrian and Trócsányi, Zoltan, *One loop radiative corrections to the helicity amplitudes of QCD processes involving four quarks and one gluon*, *Phys.Lett.* **B336** (1994) 529–536, [hep-ph/9405386].

[45] R. K. Ellis, W. Giele, Z. Kunszt, K. Melnikov, and G. Zanderighi, *One-loop amplitudes for* $W + 3$ *jet production in hadron collisions*, *JHEP* **0901** (2009) 012, [0810.2762].

[46] P. Nogueira, *Automatic Feynman graph generation*, *J.Comput.Phys.* **105** (1993) 279.

[47] J. Vermaseren, *New features of FORM*, math-ph/0010025.